Multimodal imaging as optical biopsy system for gastritis diagnosis in humans, and input of the mouse model

Thomas Bazin, Alexandre Krebs, Aude Jobart-Malfait, Vânia Camilo, Valérie Michel, Yannick Benezeth, Franck S. Marzani, Eliette Touati, Dominique Lamarque

EBioMedicine 69 (2021) 103462

Contents lists available at ScienceDirect

EBioMedicine

journal homepage: www.elsevier.com/locate/ebiom

Research paper

Multimodal imaging as optical biopsy system for gastritis diagnosis in humans, and input of the mouse model

Thomas Bazin[a,*], Alexandre Krebs[b], Aude Jobart-Malfait[c], Vania Camilo[c], Valérie Michel[d], Yannick Benezeth[b], Franck Marzani[b], Eliette Touati[d], Dominique Lamarque[a]

[a] Université Paris Saclay/UVSQ, INSERM, Infection and Inflammation, UMR 1173, AP-HP, Hôpital Ambroise Paré, Department of Gastroenterology, F92100, Boulogne-Billancourt, France
[b] ImViA EA7535, Université Bourgogne Franche-Comté, Dijon, France
[c] Université Paris-Saclay, UVSQ, Inserm U1173, Infection et inflammation, Laboratory of Excellence INFLAMEX, 78180, Montigny-Le-Bretonneux, France
[d] Unit of Helicobacter Pathogenesis, Department of Microbiology, CNRS UMR 2001, Institut Pasteur, F75724 Paris cedex 15, France

ARTICLE INFO

Article History:
Received 12 March 2021
Revised 10 June 2021
Accepted 10 June 2021
Available online 3 July 2021

Keywords:
Gastritis
Gastric cancer
Optical biopsy
Reflectance
Autofluorescence
Helicobacter pylori

ABSTRACT

Background: Gastric inflammation is a major risk factor for gastric cancer. Current endoscopic methods are not able to efficiently detect and characterize gastric inflammation, leading to a sub-optimal patients' care. New non-invasive methods are needed. Reflectance mucosal light analysis is of particular interest in this context. The aim of our study was to analyze reflectance light and specific autofluorescence signals, both in humans and in a mouse model of gastritis.

Methods: We recruited patients undergoing gastroendoscopic procedure during which reflectance was analysed with a multispectral camera. In parallel, the gastritis mouse model of *Helicobacter pylori* infection was used to investigate reflectance from ex vivo gastric samples using a spectrometer. In both cases, autofluorescence signals were measured using a confocal microscope.

Findings: In gastritis patients, reflectance modifications were significant in near-infrared spectrum, with a decrease between 610 and 725 nm and an increase between 750 and 840 nm. Autofluorescence was also modified, showing variations around 550 nm of emission. In *H. pylori* infected mice developing gastric inflammatory lesions, we observed significant reflectance modifications 18 months after infection, with increased intensity between 617 and 672 nm. Autofluorescence was significantly modified after 1, 3 and 6 months around 550 and 630 nm. Both in human and in mouse, these reflectance data can be considered as biomarkers and accurately predicted inflammatory state.

Interpretation: In this pilot study, using a practical measuring device, we identified in humans, modification of reflectance spectra in the visible spectrum and for the first time in near-infrared, associated with inflammatory gastric states. Furthermore, both in the mouse model and humans, we also observed modifications of autofluorescence associated with gastric inflammation. These innovative data pave the way to deeper validation studies on larger cohorts, for further development of an optical biopsy system to detect gastritis and finally to better surveil this important gastric cancer risk factor.

Funding: The project was funded by the ANR EMMIE (ANR-15-CE17-0015) and the French Gastroenterology Society (SNFGE).

Introduction

Globally, gastric cancer is the fifth most common cancer and the third leading cause of cancer-related death [1]. In patients with chronic inflammation of the gastric mucosa precancerous lesions may occur in one quarter of cases [2]. Tissular inflammation is most often not detectable by gastric endoscopic examination using white light. Moreover, histological analysis of systematic (non-targeted) gastric biopsies does not reflect the spread and actual severity of inflammation. Thus, new tools for wide screening of gastric inflammation are needed.

New endoscopic imaging techniques can improve the detection of gastric inflammation. The intensity of the light that is re-emitted by the illuminated mucosa, or reflectance, results from different processes (absorption, reflection, scattering, transmission, autofluorescence (AF)), which themselves depend on the wavelengths of

* Corresponding author at: Hôpital Ambroise Paré, 9 avenue Charles de Gaulle, 92100 Boulogne Billancourt, France.
E-mail address: thomas.bazin@aphp.fr (T. Bazin).

https://doi.org/10.1016/j.ebiom.2021.103462

Research in context

Evidence before this study

Gastric cancer prevention requires efficient screening of gastric inflammation. However, currently available techniques in clinical practice are not satisfactory, as they rely on histology only, leading to sampling error and underestimation of the actual degree of inflammation. Non-invasive optical biopsy systems, based on analysis of the light re-emitted by the gastric mucosa after exposing it to a light flux, are of particular interest in this indication. Very few studies analyzed the ability of re-emitted light analysis to distinguish normal from inflamed mucosa. Preliminary results suggest that total reflectance (that is all the re-emitted light) is modified in the case of gastritis.

Added value of this study

We measured re-emitted light from patients with gastritis and from healthy controls. In addition, we used the *Helicobacter pylori* mouse model of gastritis to consolidate our results. We analyzed not only total reflectance but also the autofluorescence subpart, that is the light re-emitted at higher wavelengths than the excitating light. Compared to previous studies, we extended the spectrum of excitation light to near infrared. Moreover, we used a practical and very sensitive device to measure light intensity variations. We identified reflectance modifications in near-infrared spectrum in gastritis patients, and variations of autofluorescence. In a gastritis mouse model, we also observed reflectance modifications 18 months after *Helicobacter pylori* infection in the presence of severe inflammation of the gastric mucosa, and modifications of autofluorescence after 1, 3 and 6 months.

Our findings are the first to prove that reflectance analysis is able to distinguish gastritis patients from controls with high accuracy. It is also the first to prove that autofluorescence signals are modified in the case of gastritis. Our results are reinforced by consistency with those of the mouse model.

Implications of all the available evidence

Both in humans and in mice, the reflectance data identified as discriminant for gastritis diagnosis can be considered as biomarkers of inflammation. Our results are in line with the previous ones, and clarify them. The measurement devices that we used makes the transition to real-time clinical measurements technically feasible. This will make it possible to test, prospectively, our techniques diagnosis capabilities on large validation cohorts. If our results are confirmed, current practice may change: random gastric biopsies may become unnecessary in the absence of visible lesions. This would make it possible to reduce the time and cost of numerous procedures, while making it possible to better target the samples in the event of an anomaly identified by the reflectance analysis. Moreover, our technique is easily transposable for looking for tissue inflammation in other sites such as colon in inflammatory bowel disease context.

In addition, our results pave the way for mechanistic studies, to decipher which tissue modifications are at the origin of the modifications of re-emitted light.

excitation light. The gastrointestinal tract, forming an ideal dark environment, can be explored by reflectance and AF analysis techniques. By spectrophotometry, Charvet et al. have shown that reflectance analysis is able to better identify pathological mucosa than endoscopic examination [3]. In a previous study, we demonstrated for the first time that multispectral imaging is capable to detect reflectance modifications at specific wavelengths on visible spectrum, associated with gastric inflammation, both in a mouse model and in human [4]. AF is much more difficult to acquire because it needs filtering the light before excitation and after emission. Interestingly, tissular AF properties are modified in pathological context such as inflammation, as changes occurring in tissues result in different amount and composition of endogenous fluorophores [5].

The major aim of the present study was to analyze, in the case of gastritis, the modifications of gastric reflectance in humans, using a practical and sensitive measuring device. In addition, we also analyzed the AF modifications. The relevance of gastric reflectance and AF data as potent biomarkers of the presence of inflammation was also studied in a mouse model of *H. pylori* infection, closely mimicking chronic gastritis in human pathology.

Methods

Human

Subjects

We included prospectively patients referred to the endoscopic unit of Ambroise Paré hospital, Boulogne-Billancourt, France, from ENDOSPECTRALE study (ClinicalTrials.gov identifier: NCT04287569). Patients were eligible if they had been scheduled for gastroscopy under general anesthesia and had given their written informed consent. In addition, we included retrospectively patients with chronic gastritis from the GASTRIMED cohort (ClinicalTrials.gov identifier: NCT02325323), funded by the French Gastroenterology Society (SNFGE).

We recorded multispectral videos from 27 patients, included from January 2020 to July 2020. We only kept videos which did not show any evidence of visible lesions under white light, in order to avoid re-emitted light modification due to macroscopic abnormalities such as gastric atrophy or ulcers. Of note, due to recruitment constraints and in particular the need to use a specific fixative (Carnoy), autofluorescence acquisitions were realized on biopsies from other 18 patients. These patients were recruited from June 2017 to June 2018. All patients' characteristics are summarized in Table 1. Consequently, we do not have both multispectral and autofluorescence data for any patient. *H. pylori* was observed in histological slices of only one chronic gastritis patient in both cohorts. Sex ratio and age were similar between groups.

Procedure

Multispectral acquisition. During gastroscopy, the endoscope (Olympus Exera II) was focused on the antrum. We illuminated the mucosa using a xenon lamp as the light source (1000W) equipped with a long-pass filter to prevent UV illumination, and an optical fiber as light transmitter, inserted into the working channel of the endoscope (Image 1). Reflectance light was collected by the optical fiber and analyzed by two CMOS sensors, one calibrated to measure visible spectrum (VIS, from 400 to 630 nm with a 10 nm step, reference CMV2K SSM4×4) and the other to measure the red part of visible spectrum and the near infrared spectrum (NIR, from 610 to 840 nm with a 10 nm step, reference CMV2K SSM5×5).

Image pre-processing and classification. Each gastroendoscopic video (maximal duration of 30 seconds), acquired during endoscopy procedure, was divided in images NIR and VIS with a resolution of 512×256 for VIS sensor and 409×216 for NIR sensor. Each image was filtered by a 7×7 low-pass filter to eliminate noise and we then selected the pixels arranged on a regular grid by taking 1 pixel out of

Table 1
Characteristics of the patients included in the study. Values reported for inflammatory infiltrates, lymphocytes, Polynuclear neutrophils correspond to histological mean scores grading (means +/- SD).

	Sex ratio F/M	Age	Infiltrate location	Lymphocytes	Polynuclear neutrophils	Total histological score	Hp positive
Patients used for multispectral analysis							
Chronic gastritis (n=16)	1.1	57.3 +/- 19.9	1.8 +/- 0.2	1.1 +/- 0.6	0.1 +/- 0.3	3.0	1
Controls (n=11)	0.5 (NS)	54.8 +/- 14.6 (NS)	0.0 +/- 0.0	0.0 +/- 0.0	0.0 +/- 0.0	0.0	0
Patients used for AF analysis							
Chronic gastritis (n=3)	2	41.3 +/- 13.5	2 +/- 0.0	1.3 +/- 0.6	1.0 +/- 0.0	4.3	1
Controls (n=15)	0.3 (NS)	50.8 +/- 15.9 (NS)	0.4 +/- 0.5	0.4 +/- 0.5	0 +/- 0.0	0.8	0

7 horizontally and vertically. In order to avoid under- or over-exposure, only pixels with intensity values between 128 and 512 have been kept. We analyzed 100 pixels by patient. We applied a L1 type normalization for each pixel: all the values were expressed as a ratio of the total intensity per pixel. We reduced data dimensionality using a principal component analysis and then used a simple SVM classifier with a linear kernel. In order to assess the diagnosis properties of multispectral data for gastritis, we used a "leave one patient out" method, as described in a previous study [6]. Diagnostic properties of all the tests were aggregated on a confusion matrix and represented on ROC curve.

Biopsy collection. After multispectral acquisition we performed systematic biopsy collection from the antrum and the corpus, according to standard protocols. These biopsies were placed in 10% formalin and in Carnoy for AF analysis, and embedded in paraffin. Transversal gastric tissue section samples were stained by hematoxylin and eosin (H&E) for routine histological analysis. In addition, immunochemistry using Dako polyclonal rabbit IS523 (Dako, Glostrup, Denmark) was performed to detect *H. pylori* infection. Biopsies were scored for the severity of inflammatory lesions according to the Updated Sydney System [7]. The histopathological diagnosis was performed by a senior pathologist (CJ). The patients were separated into two clinical groups based on histology analysis: patients with a total score > 2 were considered as "chronic gastritis" patients.

Tissue autofluorescence acquisition. Autofluorescence was measured under sequential illumination between 470 and 670 nm on 6 μm-thick dewaxed sections of paraffin blocs from biopsy collection, using a Leica TCS SP8 AOBS spectral confocal microscope (Heidelberg, Germany). The excitation wavelength was changed every 10nm and emission wavelength band pass was 20nm. Laser excitation power was set to the same power for each excitation wavelength. The setup is described in Fig. 1. For each sample, we performed 6 acquisitions with a 63x objective (field-of view size: 184*184 μm). Each acquisition is constituted of a matrix of 211 intensities values corresponding to 211 excitation/emission couples. The 6 matrices acquired per sample were averaged to obtain only one matrix per sample.

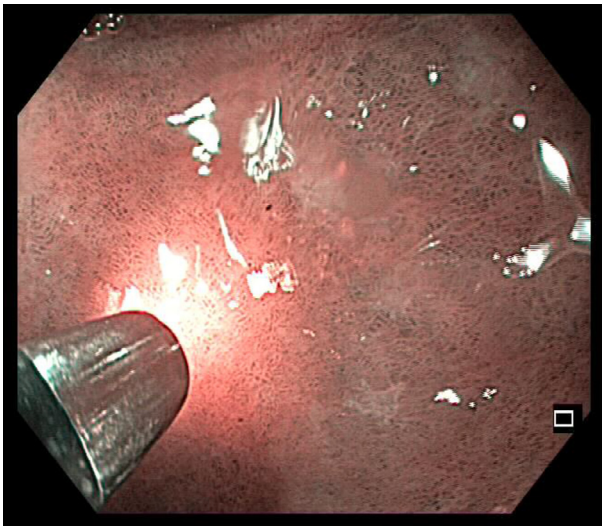

Image 1. Gastric mucosa illumination via the optical fiber inserted into the endoscope. The black part corresponds to the optical fiber protected by a sheath. The metallic part corresponds to the distal end of the fiber. The luminous flux, directed by the optical fiber, illuminates the gastric mucosa. The re-emitted light is transmitted in the opposite direction by the optical fiber to the sensor.

Mouse model

Bacterial strains and growth conditions

The *H. pylori* strain SS1, able to colonize the mouse gastric mucosa for long periods [8], was used in this study. Bacteria were grown on blood agar base 2 (Oxoid Lyon, France) plates supplemented with 10% defibrinated horse blood (bioMérieux, Marcy L'Etoile, France) and an antibiotic-antifungal mixture consisting in vancomycin (10mg/ml), polymyxin B (2.5 IU/l), trimethoprim (5mg/ml) and amphotericin B (4mg/ml). The plates were incubated at 37°C for 24h to 48h under microaerobic conditions (7% O2, 10% CO2; Anoxomat system).

Mouse infection

Sixty C57BL/6 male mice of 5-6 weeks-old (Charles River Laboratories; France) were included in the study. Mice were acclimatized for one week before starting the experiments. Thirty mice were orogastrically inoculated with 150μl of a suspension of the *H. pylori* strain SS1 (10^8 colony forming unit (CFU)/ml) [8]. In parallel, thirty non-infected mice received 150μl of peptone broth. After 1, 3, 6, 12 and 18 months (M1, M3, M12 and M18 respectively) 6 infected and 6 non-infected mice were sacrificed, their stomach isolated and

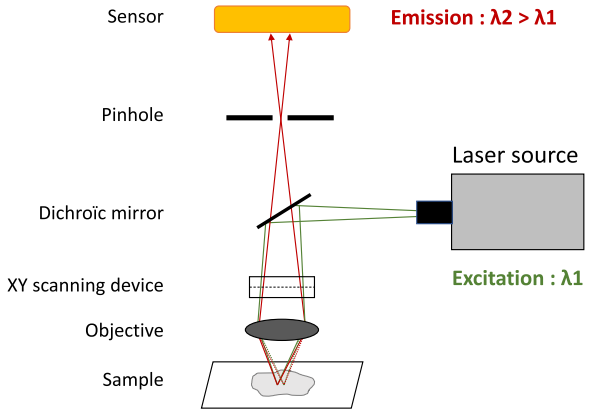

Fig. 1. Confocal laser scanning microscope setup. Excitation light (green line) is produced by a laser source, reflected by a mirror and focalized by a lens on the sample. The XY scanning device allows imaging of large sample areas. The re-emitted light (red line) passes through the pinhole and is detected by the detector. AF component is defined as light emitted at wavelengths longer than the excitation light.

fragments were used for histology, reflectance spectra and autofluorescence analysis. In addition, *H. pylori* gastric inoculation was performed as previously described [9].

Histological analysis

Stomach samples were fixed in RCL2 (Alphelys, France) and embedded in paraffin. Six μm-thick sections were stained by H&E and examined blindly for lymphocytes and polynuclear neutrophil infiltration, which were semi-quantitatively evaluated as previously described [10,11], based on a scoring system with four severity grades (0= none, 1: mild, 2: moderate, 3: severe) according to the Updated Sydney System [7]. Mice and human samples were thus graded according to the same score. B lymphocytes infiltration was visualized by anti-CD45R immunostaining (BD 550286, 1/100, BD Biosciences, RRID: AB_393581) on mice gastric tissue section at M18.

Tissue reflectance

The reflectance of the mucosa was measured using a spectrometer Avantes AvaSpec-ULS2048L, which retrieves the reflectance of the measured surface (1cm diameter disk) from 200 nm to 1160 nm, with a 0.597nm resolution (1315 measurements). A median of six acquisitions by samples were performed using the software supplied with the spectrometer. We averaged and normalized the spectra in order to obtain one spectrum for one timepoint in each group. We used an integrating sphere with a halogen light source (AvaSphere-50-LS-HAL-12V, 5W) to illuminate the tissue homogeneously with diffuse light.

Tissue autofluorescence

AF was measured as described above for human, using 6 μm-thick dewaxed sections of paraffin blocs from stomach biopsies collection.

Ethics

This ENDOSPECTRALE study for the human part was approved by the Comité de Protection des Personnes Sud-Est III ethics committee on June 2019 (EudraCT number: 2019-A01602-55). The study was conducted according to the World Medical Association Declaration of Helsinki. GASTRIMED cohort was approved by the Comité de Protection des Personnes MS1 ethics committee on April 2014 (reference number: 13059).

Mouse experiments were carried out in strict accordance with European recommendations. The protocol has been approved by the Committee of Central Animal Facility Board, the Ethic committee on animal experimentation of the Institut Pasteur (Ref. 2013-0051) and the French Ministry of Higher Education and Research (Ref. 00317.02).

Statistics

In order to compare, on one hand, the differences on the reflectance spectra, and on another hand, on AF spectra between the two groups: gastritis patients *vs* controls for human and infected *vs* non-infected for mice, we performed parametric Student t-test after confirmation of data normal distribution using Shapiro test. We applied Benjamini-Hochberg correction on the normalized spectra from spectrometer and from confocal microscope; α risk was set at 0.05. Of note, we corrected AF p-values for the number of couple excitation-emission that varied of more than 5% between gastritis group and controls. Raw data are available as supplementary data.

No power analysis was used as no robust hypothesis concerning our evaluation criteria exist. We determined the sample size according to the recruitment capacities in our clinical center, and according to the ANR budget for the mouse model.

Role of funders

The study sponsors had no role in the study.

Results

Human

Multispectral analysis in human

Multispectral videos were recorded on 27 patients during gastric endoscopy. 16 patients were classified as chronic gastritis patients, 11 as controls. Consequently, 2700 spectra were analyzed in total. The spectral profile from the visible (VIS) sensor was similar in chronic gastritis patients and in controls (Fig. 2a). At the opposite, red and near-infrared (NIR) sensor showed differences in chronic gastritis patients compared to controls, with decreased intensity before 740 nm and increased intensity after (Fig. 2b). These differences were statistically significant, after correction for multiple testing, between 610 and 725 nm and between 750 and 840 nm. Median spectra by patient showed a clear grouping of spectra in red and near-infrared, with a spindle look (Fig. 2d), contrary to visible spectra (Fig. 2c).

Principal component analysis showed a clustering of patients, as mainly two groups are well distinguished, chronic gastritis and controls (Fig. 3a). Two principal discriminant components were identified, and used by the classifier to distinguish the two groups. ROC curve testing the gastritis diagnosis properties of the combination of wavelengths identified as discriminant by the classifier showed an AUC of 0.83, with a Se of 79% and a Spe of 80% using the best compromise (Fig. 3b).

AutofluoresCence

The results of matrices comparison in gastritis patients defined as inflammation grading $>$ 3 on biopsies (n=3) versus control (n=15) are presented in Fig. 4. Two zones were statistically different: the emission zone between 532 nm and 574 nm (excitation between 500 nm and 540 nm) with a decreased intensity in gastritis patients, and the emission zone between 563 nm and 690 nm (excitation at 480, 500 and 510 nm) with an increased intensity in gastritis patients, compared to controls.

Mouse

In order to investigate whether spectral and AF variations observed in humans, are also relevant on well-defined gastric inflammatory lesions as observed in long-term chronically *H. pylori*-infected mice, we acquired reflectance spectra and AF at different time-points of infection on the mice gastric mucosa.

The presence of *H. pylori* was confirmed at each time-point by the measure of gastric colonization (Fig. 5b). No H. pylori colonization was observed in the non-infected control groups (not shown).

Histological inflammation score was obtained at each time-point of infection. No inflammation was observed on non-infected mice whatever the timepoint, and on infected mice at M1. At M3, all infected animals exhibited a mild focal inflammation of the gastric mucosa and/or submucosa, associated with minimal focal hyperplastic lesions in 2/6 animals. From M6, a moderate to severe inflammation including polynuclear neutrophils (PMN) infiltrate was observed in infected animals, predominantly in the submucosa. At M12 and M18 lymphocyte aggregates were visible in submucosa. At M18 we observed an elongation of gastric pits, with oedema and intestinal metaplasia (Fig. 6). CD45 immunohistochemical staining was positive in infiltrate at M18, in favor of B lymphocytes infiltration (Fig. 5c). Means of inflammation scores

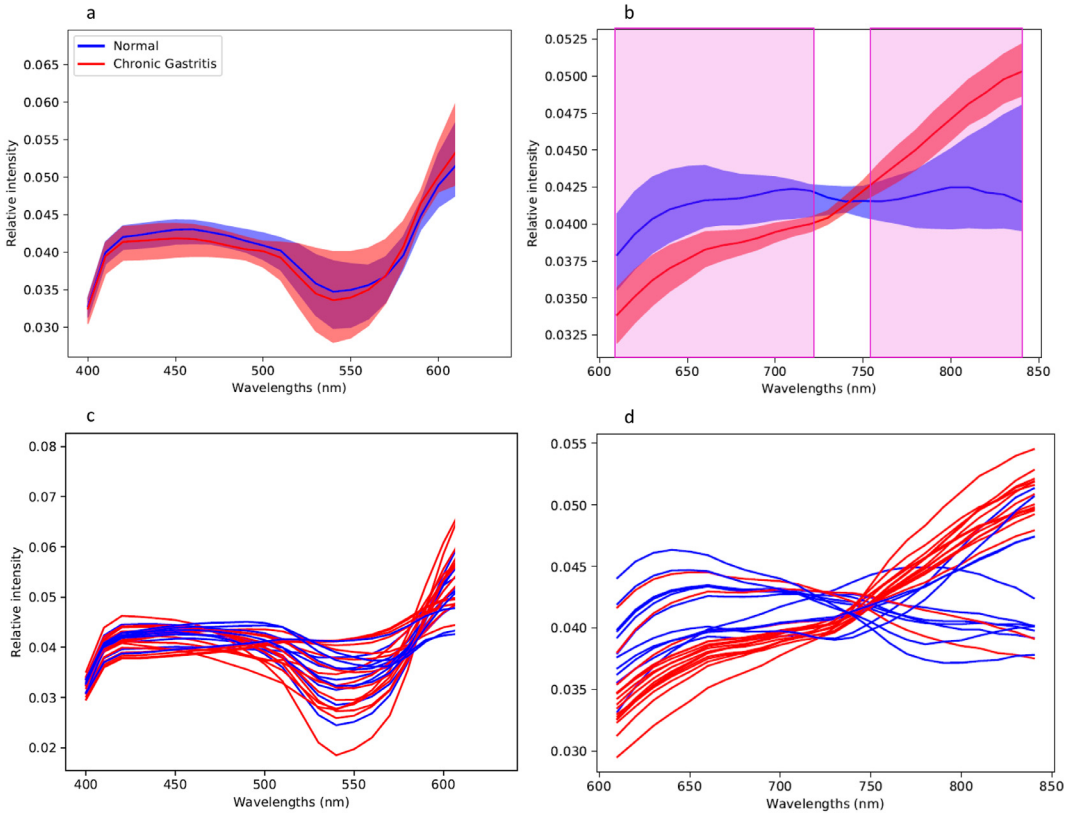

Fig. 2. Spectral profiles in visible spectrum (a and c) and in red and near infrared (b and d). For a and b, values are means of relative intensities +/- SD (light colors). Pink rectangle = wavelength band statistically different between controls and chronic gastritis patients. For c and d, values are medians of relative intensities per patients, each curve corresponding to one individual. Normal mucosa: n = 11, gastritis, n = 16.

for the grading of lymphocytes and PMN are presented in Fig. 5a, showing a significantly increased with the time of infection.

Multispectral analysis

The reflectance data were expressed as relative intensity. At M1, M3 (Fig. 7A), M6 and M12 (see Supplementary material) following infection no change was observed in infected mice compared to controls. At 18 months a significant increase in reflectance was observed in infected mice (n = 6) on all wavelengths from 617 to 672 nm compared to controls (n = 6) (Fig. 7B). We used the intensity at 654 nm as a biomarker of *H. pylori* gastritis, this wavelength being located in the middle of the significantly different wavelength band between infected and uninfected mice. The AUC of the ROC curve was 0.95 (Fig. 7C), showing excellent diagnostic performance for a threshold of 0.1% relative intensity compared to the whole spectrum (Se = 71%, Spe = 89%).

Autofluorescence

Significant modifications in autofluorescence on histological section of infected mice compared to controls was observed (Fig. 8), notably between 542 and 573 nm at M1 (excitation at 500 nm), M3 (excitation between 490 and 520 nm) and M6 (excitation between 500 and 520 nm) and between 605 and 657 nm at M3 (excitation between 510 and 580 nm). None of these changes were correlated with inflammation grading or inflammation sub-scores. At M12 and at M18 no significant changes were observed.

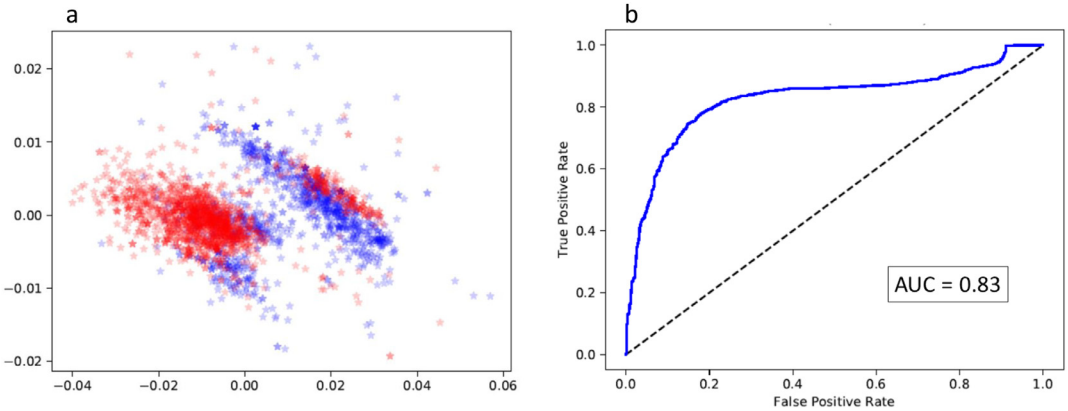

Fig. 3. Groups differentiation using multispectral data. a. Principal component analysis with projected data along the two first components. Chronic gastritis patients' data are represented by red symbols, controls data by blue symbols. **b.** ROC curve representing the gastritis diagnosis properties of multispectral data. Normal mucosa: n = 11, gastritis, n = 16.

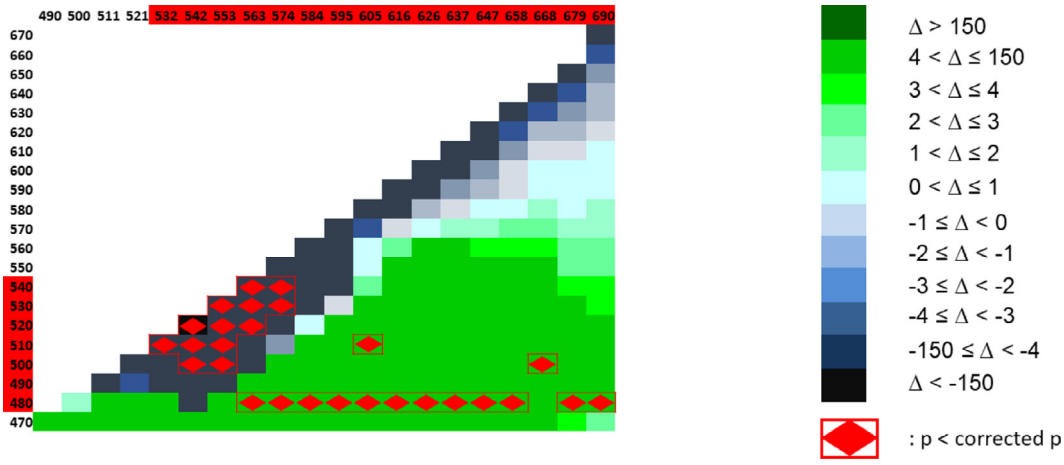

Figure 4. Comparison of autofluorescence matrices obtained from gastric biopsies in patients and in controls; x-axis: emission wavelengths; y-axis: excitation wavelength; Δ: normalized average intensity in gastritis patients − normalized average intensity in controls; corrected p: Benjamini-Hochberg correction applied to 0.05 α risk, Student's t-test. Normal mucosa: n = 15, gastritis, n = 3.

Discussion

There is an important clinical requirement to improve imaging and screening method for gastric inflammatory lesions, recognized as the first steps in the gastric cancer process. To our knowledge, there is no technology capable of exploring large areas of gastric tissue during an endoscopic examination to detect gastritis. In this study, we observed both in humans and in the gastritis mouse model, that reflectance and autofluorescence are modified in the case of gastritis. In both models, reflectance spectra data were capable to accurately predict the histological inflammatory state. As previously suggested [12], our data also support that these techniques can thus be integrated in the wider range of analytical procedures known as *Optical biopsy* (or *Virtual Chromo Endoscopy*), allowing the obtention of gastric inflammation diagnosis *in vivo*, non-invasively, without the need of biopsies or the administration of exogenous markers.

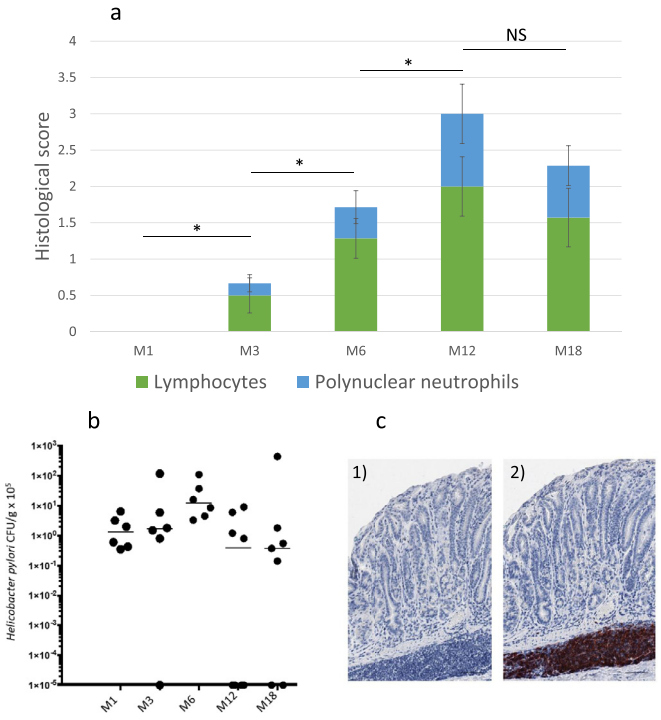

Fig. 5. Evolution of inflammation and infection overtime in mice. a. Evolution of score grading of gastric inflammation induced by *H. pylori* infection in mice after 1 (M1), 3 (M3), 6 (M6), 12 (M12) and 18 (M18) months post-infection. Values are means of histological score ± SEM. *: $p<0.05$; NS: non-significant (Student's t-test). b. *H. pylori* gastric colonization over time; n = 6 at each timepoint; bar = median. c. CD45 immunohistochemical staining in glandular part of the stomach at M18 on mice. 1) Control mouse. 2) Infected mouse. Note the positivity of the staining in monocellular infiltrate localized in submucosa in infected mouse. *Scale bar = 50 μm.* At each timepoint, non-infected mice: n = 6, infected mice: n = 6.

Re-emitted light has already been studied to detect tissular inflammation. The most advanced technique available is confocal laser endomicroscopy. This technique is able to assess tissular structure and correlates well with inflammatory scores in the colon [13] and in the stomach [14–16], but it requires extra material, injection of exogeneous marker, is highly time-consuming, may induce allergic reaction, and concerns only millimeter-scale portions of mucosa. In a reflectance study by Charvet et al., the authors exposed the mucosa to visible and NIR spectrum (490-950 nm), using an optical multifibers mini probe inserted into the biopsy channel of the endoscope, and connected to a spectrometer. They observed that optical coefficients (absorption and scattering coefficients) distinguished normal from pathological mucosa. However, basal light intensities did not differ depending on the inflammation severity [3].

In the present study, spectrometer measurements in mouse and multispectral data in human confirmed significant modifications in red spectrum that we observed in our previous study [4], with light intensity at 640 nm associated with gastritis. As previously suggested, collagen network modifications and hemoglobin oxygen saturation may explain these results [4]. However, we did not find significant differences at 560 and 600 nm, contrary to our previous findings. It is important to highlight that our reflectance results go further than those previously observed, as the reflectance spectrum in the current study is broader and the system more accurate: we used dedicated sensors to separate spectra in wavelengths bands when in the previous study we filtered excitation light. Thanks to these improvements, we observed significant modifications in near infrared spectrum in human, for the first time to our knowledge. Differences between our results and previous data may be due to the different gastritis threshold considered, corresponding to a Sydney score > 2, in the present study. Importantly, we used a specific device with an optical fiber compatible with endoscopes used in clinical practice. Our device is thus easily transposable to routine care.

A major challenge concerning reflectance data analysis acquired in vivo is to deal with a huge amount of information, with an important part of non-informative data due to the specificity of gastroendoscopic video acquisition such as rapid movements of the endoscope,

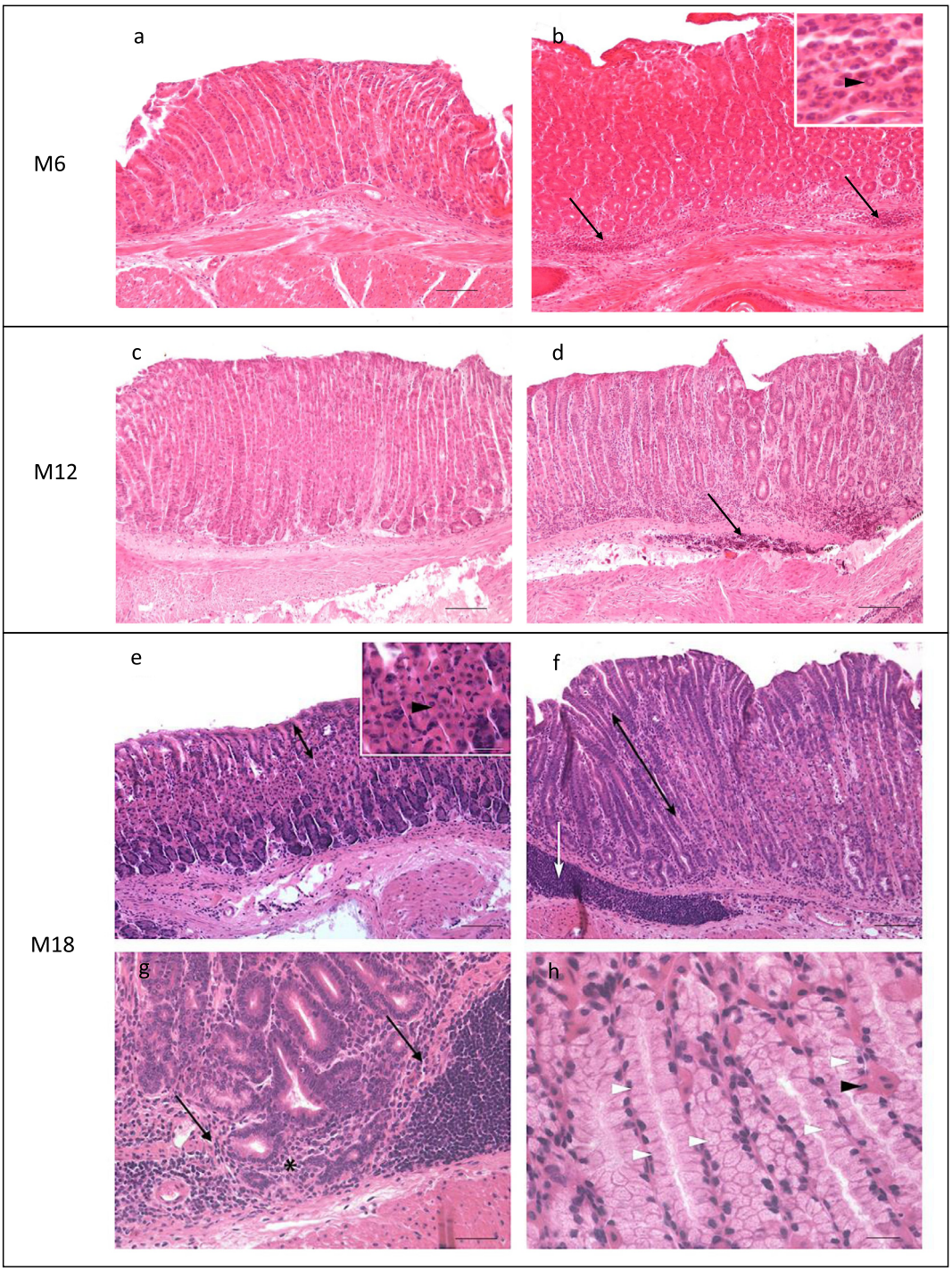

Fig. 6. Gastric histologic lesions overtime post-*Helicobacter pylori* infection in the mouse model. H&E staining. Glandular part of the stomach. *Scale bar = 50 μm unless otherwise stated.* **a.** Control mouse at M6. **b.** Infected mouse at M6. Large infiltrates of polynuclear neutrophils (black arrows and insert, black arrowhead, *scale bar = 10 μm*). **c.** Control mouse at M12. **d.** Infected mouse at M12. Large infiltrates of lymphocytes (black arrow). **e.** Control mouse at M18. Note the short gastric pits (black double arrow) – *Scale bar = 100 μm.* **Inset:** focus on fundic glands; most of the cells are large, roundish with a pink granular cytoplasm and a central round nucleus (parietal cells, black arrowhead) – *Scale bar = 20 μm.* **f.** Infected mouse at M18. Note the focal elongation of gastric pits (foveolar hyperplasia, black double arrow). Large infiltrates of small lymphocytes (probably a hyperplasia of the Mucosa Associated Lymphoid Tissue) were detected in the submucosa (white arrow). **g.** Infected mouse at M18. Focal rupture of the *muscularis mucosae* (black arrows), with glands observed in the submucosa (herniation?). Note the oedema associated with the infiltration of the *lamina propria* (asterisk) by lymphocytes, plasma cells and few macrophages. **h.** Infected mouse at M18. In contrast to control mice, parietal cells were almost completely replaced by mucus cells (intestinal metaplasia, white arrowheads) – *Scale bar = 20 μm.*

digestive peristalsis, and the presence of artefacts (bubbles, mucus). We computed our data with a specific classification pipeline, obtaining excellent diagnosis properties on in silico auto-validation cohort. These steps are easily integrable in a dedicated software and can be dealt real-time using a top-level processor. A full integrated setup is the next logical step.

Trimodal imaging combining white-light endoscopy, AF imaging and narrow-brand imaging has already been described [17,18], but this technique has never been applied for inflammation detection in stomach. This device uses excitation light between 390 and 470 nm at the limit of the visible while the re-emission was arbitrarily and globally captured between 500 and 630 nm. Consequently, it can only detect the

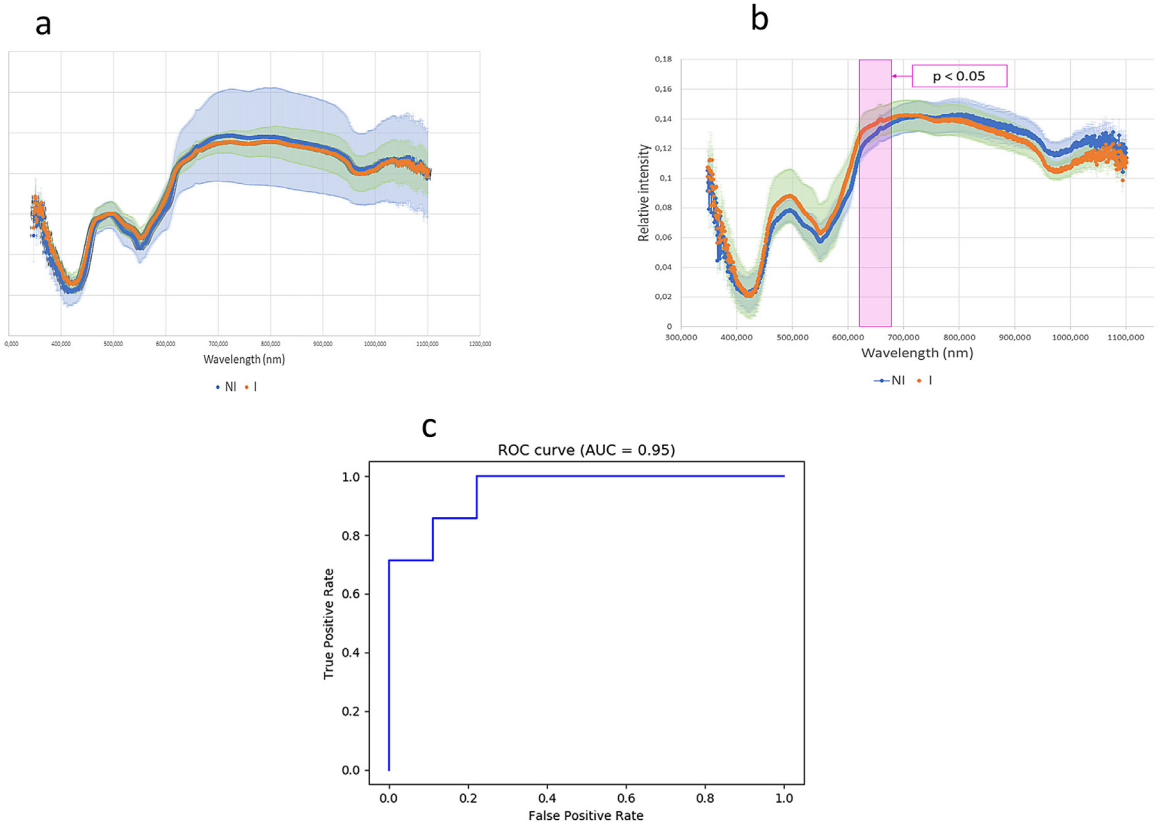

Fig. 7. Multispectral analysis in mouse. a. Mean reflectance spectra at M3. NI: non-infected mice; I: infected mice; light blue = SD for NI; light green = SD for I. b. Mean reflectance spectra at M18. Pink rectangle = wavelength band statistically different between NI and I. **c.** ROC curve for light intensity at 654nm as a biomarker to discriminate controls from infected mice 18 months after *Helicobacter pylori* infection. At each timepoint, non-infected mice: n = 6, infected mice: n = 6.

emission of certain fluorophores, mainly collagen. Our method, although carried out *in vitro*, experimentally sought the reemission of other fluorophores from an excitation between 470 and 670 nm and a detection by fine spectral bands between 500 and 700 nm.

Some AF data are available concerning colonic inflammation. Green component was observed as inversely correlated with colonic inflammation severity in ulcerative colitis [19], that is wavelengths between 490 et 573 nm (AFNOR X08-010), compatible with our findings. In a similar prospective study by Moriichi et al., investigating a link between autofluorescence (measured between 500 and 630 nm) and colic inflammation in ulcerative colitis, global fluorescence intensity was found to be inversely correlated with colonic inflammation [20]. The authors concluded that AF can be considered as an objective indicator of colitis, especially for less-experienced endoscopists. Wizenty et al. found more pronounced AF in histological slices of inflamed colonic mucosa from mice and human, at

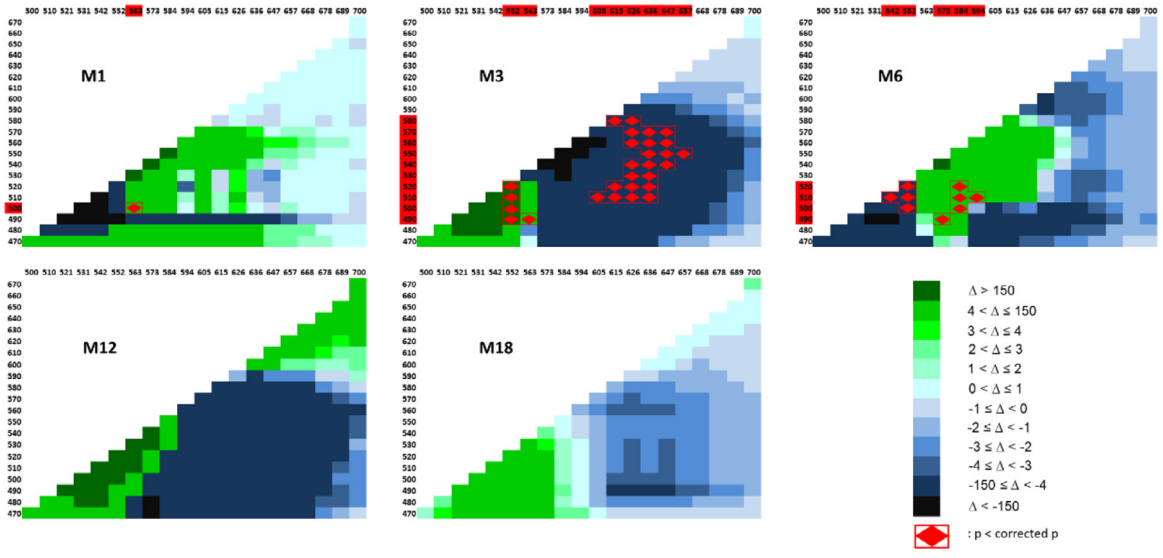

Fig. 8. Comparison of autofluorescence matrices overtime in infected and non-infected mice; x-axis: emission wavelengths; y-axis: excitation wavelength; Δ: normalized average intensity in infected mice − normalized average intensity in non-infected mice; corrected p: Benjamini-Hochberg correction applied to 0.05 α risk, Student's t-test. At each timepoint, non-infected mice: n = 6, infected mice: n = 6.

emission spectra between 424 nm and 738 nm [5]. At our knowledge, no AF data exist concerning gastritis.

Concerning our AF analysis in human, our gastritis group was small because we chose the threshold of 3 (>2) for Sydney score to define gastritis, which excluded mild gastritis. As this score is realized a posteriori, after the inclusion, it was not possible to balance groups due to recruitment constraints. Despite of the small size of this group (3 patients), results were statistically significant after stringent multiple testing correction, this being in favor of major differences.

The AF differences are significant in mice only at the first timepoints, with no differences at M12 and M18. Moreover, the intensity in autofluorescence matrices did not vary in the same direction overtime in mouse and between mouse and human, may be due to the intrinsic gastritis differences between these two organisms, thus making comparison and results interpretation difficult. In both models, an important limitation of our study is that AF analysis has been performed on biopsies, that do not integrate some important aspects compared to *in vivo* (water content, oxygen saturation etc.).

In mice, we did not observe an overlap between modified AF and multispectral data, as differences in AF were visible only at early timepoints while multispectral spectra were different only later at M18. We did not perform AF and multispectral analysis on the same patients, which makes it impossible to determine the part of autofluorescence in the global multispectral signal in humans. However, as AF light intensities are much lower than global re-emitted light intensities, AF modifications contribution to global multispectral spectra is probably limited.

We did not expect the reflectance and AF changes to be similar between mice and humans, as mouse gastritis model has its limitations *per se*, mainly due to the histological particularities of gastritis in mouse which is not diffuse as observed in humans and also to the time constraints of mice experiments leading to a chronic gastritis in the presence of *H. pylori* infection but on a shorter period of time compared to humans. In particular, we observed in infected mice as previously described [21], a basal lymphocytic infiltration near the muscular layer in the sub-mucosa, while cellular infiltrate in human is diffuse.

Intestinal AF signals are due to the presence of several fluorophores [5]. Our excitation light wavelengths range restricts the number of fluorophores that could explain our AF spectra, as collagen for instance produces AF only when excited at lower wavelengths [12]. Finally, only three fluorophores could be involved in AF modifications observed. Lipofuscin or lipofuscin like lipopigment [22], a major AF source in immune cells [23], re-emits light over a broad spectrum, from 480 to 700 nm. Flavins AF spectra exhibits an emission peak around 550 nm. Flavins are co-factors of numerous enzymes including inducible nitric oxide synthase (iNOS) [24], a key mediator of immune activation and inflammation [21,25,26]. Only porphyrins as hemoglobin, a metalloporphyrin, could be involved in AF modifications observed in patients after 595 nm and in mice after 626 nm. Of note, as the AF acquisition window is limited to mucosa, AF modifications observed are unlikely due to blood hemoglobin. But hemoglobin expression is not limited to erythroid cells, and has been described in a variety of cell types including macrophages and epithelial cells [27]. In addition, heme is a nutritionally derived macromolecule present in the intestinal lumen in meat eating species. It is metabolized by heme oxygenase-1, that plays a central role in the regulation of epithelial inflammation [28] and is inducible by inflammatory context [29]. The tissue concentration can therefore decrease in the event of inflammation.

Despite the difficulties to correlate the AF modifications observed with specific variation of some mucosal components during the inflammatory process, the modifications are significant in wavelength zones corresponding to endogenous fluorophores spectra, which supports the biological relevance of our data and the method we developed.

Altogether, these results point to the fact that we do not have simultaneous in vivo measurements of total reflectance and AF, which would be the only way to decipher the contribution of AF in in vivo reflectance modifications.

Our results show that dedicated analysis of reflectance from gastric mucosa can detect inflammation not visible to the human eye, regardless of its severity. This analysis method is non-invasive, does not require the use of any labelling, can be performed real-time on large areas of organs and can be automated. Our study clarifies the previous results, using more precise devices that can, in humans, be used in routine clinical practice. These results testify to the interest of the development of multispectral imaging in digestive endoscopy for the detection of inflammatory lesions. The next step will be to design a fully-integrated setup with real-time data analysis ability, in order to test prospectively our technique diagnosis skills on large validation cohorts. In this pilot study based on reflectance and AF analysis, we observed significant modifications able to effectively predict inflammatory lesions in humans and in a mouse model of *H. pylori* gastritis. These results pave the way for the development of new endoscopic tools for the non-invasive detection of gastritis in order to optimize gastric cancer prevention.

Contributors

TB contributed to the conception of the work, to the analysis and interpretation of data, and drafted the work. AK contributed to the conception of the work, to the analysis of data, and revised the work. AJM contributed to the conception of the work, to the acquisition, analysis and interpretation of data, and revised the work. VC and VM contributed to the acquisition of data and revised the work. YB, FM, ET and DL contributed to the conception of the work, to the analysis and interpretation of data, and critically revised the work. TB, AK, ET and DL verified the underlying data. All authors read and approved the final version of the manuscript.

Supplementary material

AF images vs histology in mouse and in human.
Reflectance spectra in mouse at M1, M6 and M12.

Declaration of Competing Interest

Authors have no conflicts of interest to declare.

Acknowledgments

The project including ENDOSPECTRALE study was funded by the ANR EMMIE (ANR-15-CE17-0015), and the French Gastroenterology Society (SNFGE) funded the GASTRIMED cohort (DL).

We thank Félicie Costantino (Inserm, Montigny-Le-Bretonneux, France) for her help with the statistical analysis, Gregory Jouvion and Marine Le Dudal (Institut Pasteur, Paris, France) for mice histology figures and Richard Wheeler (Institut Pasteur, Paris, France) for reading the manuscript.

We thank the Cymages imaging facility (Université Versailles Saint-Quentin-en-Yvelines, UFR Santé-Simone Veil, Montigny-le-Bretonneux, France) and the Histology facility of the Institut Pasteur, Paris, France.

Supplementary materials

Supplementary material associated with this article can be found in the online version at doi:10.1016/j.ebiom.2021.103462.

References

[1] Bray F, Ferlay J, Soerjomataram I, Siegel RL, Torre LA, Jemal A. Global cancer statistics 2018: GLOBOCAN estimates of incidence and mortality worldwide for 36 cancers in 185 countries. CA Cancer J Clin 2018;68(6):394–424.

[2] CR 8- Kapadia. Gastric atrophy, metaplasia, and dysplasia: a clinical perspective. J Clin Gastroenterol 2003:36–9.

[3] Charvet I, Ory G, Thueler P, Brundler M-A, Saint-Ghislain M, Azarpey N, et al. Diagnosis and grading of gastritis by non-invasive optical analysis. Eur J Gastroenterol Hepatol 2004;16(11):1189–98.

[4] Bazin T, Martinez-Herrera SE, Jobart-Malfait A, Benezeth Y, Boffety M, Julié C, et al. Multispectral imaging detects gastritis consistently in mouse model and in humans. Sci Rep 2020;10(1):1–10.

[5] Wizenty J, Ashraf MI, Rohwer N, Stockmann M, Weiss S, Biebl M, et al. Autofluorescence: A potential pitfall in immunofluorescence-based inflammation grading. J Immunol Methods 2018;456:28–37.

[6] Krebs A, Benezeth Y, Bazin T, Marzani F, Lamarque D. Pre-Cancerous Stomach Lesion Detections with Multispectral-Augmented Endoscopic Prototype. Appl Sci 2020 Jan;10(3):795.

[7] Dixon MF, Genta RM, Yardley JH, Correa P. Classification and grading of gastritis. The updated Sydney System. Int Workshop Histopathol Gastritis Houst 1994;20:1161–81.

[8] Lee A, O'Rourke J, Ungria MD, Robertson B, Daskalopoulos G, Dixon MF. A standardized mouse model of Helicobacter pylori infection: Introducing the Sydney strain. Gastroenterology 1997;112(4):1386–97.

[9] Ferrero RL, Cussac V, Courcoux P, Labigne A. Construction of isogenic urease-negative mutants of Helicobacter pylori by allelic exchange. Journal of bacteriology 1992;174(13):4212–7.

[10] Prophet EB, (U.S.) AFI of P. Laboratory methods in histotechnology [Internet]. American Registry of Pathology; 1992. Available from: https://books.google.fr/books?id=R1xrAAAAMAAJ

[11] Eaton KA, Radin MJ, Krakowka S. An Animal Model of Gastric Ulcer Due to Bacterial Gastritis in Mice. Vet Pathol Online 1995;32(5):489–97.

[12] Ac C, G B. Autofluorescence spectroscopy and imaging: a tool for biomedical research and diagnosis. Eur J Histochem EJH 2014;58(4):2461.

[13] Rahmi G, Coron E, Perrod G, Levy M, Moreau J, Moussata D, et al. Probe-based confocal laser endomicroscopy for in vivo assessment of histological healing in ulcerative colitis: development and validation of the ENHANCE index. J Crohns Colitis 2020.

[14] Wang P, Ji R, Yu T, Zuo X-L, Zhou C-J, Li C-Q, et al. Classification of histological severity of Helicobacter pylori-associated gastritis by confocal laser endomicroscopy. World J Gastroenterol 2010;16(41):5203–10.

[15] Yu X, Chen J, Zheng L, Song J, Lin R, Hou X. Quantitative Diagnosis of Atrophic Gastritis by Probe-Based Confocal Laser Endomicroscopy. BioMed Res Int 2020;2020:9847591.

[16] Liu T, Zheng H, Gong W, Chen C, Jiang B. The accuracy of confocal laser endomicroscopy, narrow band imaging, and chromoendoscopy for the detection of atrophic gastritis. J Clin Gastroenterol 2015;49(5):379–86.

[17] Curvers WL, Alvarez Herrero L, Wallace MB, Wong Kee Song L-M, Ragunath K, Wolfsen HC, et al. Endoscopic tri-modal imaging is more effective than standard endoscopy in identifying early-stage neoplasia in Barrett's esophagus. Gastroenterology 2010;139(4):1106–14.

[18] Wizenty J, Schumann T, Theil D, Stockmann M, Pratschke J, Tacke F, et al. Recent Advances and the Potential for Clinical Use of Autofluorescence Detection of Extra-Ophthalmic Tissues. Molecules [Internet] 2020;25(9) [cited 2020 Dec 8] Available from: https://www.ncbi.nlm.nih.gov/pmc/articles/PMC7248908/.

[19] Osada T, Arakawa A, Sakamoto N, Ueyama H, Shibuya T, Ogihara T, et al. Autofluorescence imaging endoscopy for identification and assessment of inflammatory ulcerative colitis. World J Gastroenterol 2011;17(46):5110–6.

[20] Moriichi K, Fujiya M, Ijiri M, Tanaka K, Sakatani A, Dokoshi T, et al. Quantification of autofluorescence imaging can accurately and objectively assess the severity of ulcerative colitis. Int J Colorectal Dis 2015;30(12):1639–43.

[21] Touati E, Michel V, Thiberge J-M, Wuscher N, Huerre M, Labigne A. Chronic Helicobacter pylori infections induce gastric mutations in mice. Gastroenterology 2003;124(5):1408–19.

[22] Croce AC, Bottiroli G. Autofluorescence Spectroscopy and Imaging: A Tool for Biomedical Research and Diagnosis. Eur J Histochem EJH [Internet] 2014;58(4) [cited 2021 Jan 7] Available from: https://www.ncbi.nlm.nih.gov/pmc/articles/PMC4289852/.

[23] Vida C, de Toda IM, Cruces J, Garrido A, Gonzalez-Sanchez M, De la Fuente M. Role of macrophages in age-related oxidative stress and lipofuscin accumulation in mice. Redox Biol 2017;12:423–37.

[24] Cinelli MA, Do HT, Miley GP, Silverman RB. Inducible nitric oxide synthase: Regulation, structure, and inhibition. Med Res Rev 2020;40(1):158–89.

[25] Suschek CV, Schnorr O, Kolb-Bachofen V. The role of iNOS in chronic inflammatory processes in vivo: is it damage-promoting, protective, or active at all? Curr Mol Med 2004;4(7):763–75.

[26] Tiwari SK, Shaik AS, Shaik AP, Alyousef AA, Bardia A, Habeeb MA, et al. Gene expression patterns of COX-1, COX-2 and iNOS in H. Pylori infected histopathological conditions. Microb Pathog 2019;135:103634.

[27] Saha D, Patgaonkar M, Shroff A, Ayyar K, Bashir T, Reddy KVR. Hemoglobin Expression in Nonerythroid Cells: Novel or Ubiquitous? Int J Inflamm [Internet] 2014 2014 [cited 2021 Mar 2] Available from: https://www.ncbi.nlm.nih.gov/pmc/articles/PMC4241286/.

[28] Onyiah JC, Schaefer REM, Colgan SP. A Central Role for Heme Oxygenase-1 in the Control of Intestinal Epithelial Chemokine Expression. J Innate Immun 2018;10(3):228–38.

[29] Kikuchi G, Yoshida T, Noguchi M. Heme oxygenase and heme degradation. Biochem Biophys Res Commun 2005;338(1):558–67.